STUDY OF THE DYNAMICS OF FLUX TRAPPING IN DIFFERENT SRF MATERIALS

F. Kramer*, S. Keckert, O. Kugeler, J.Knobloch[1], Helmholtz-Zentrum Berlin, Berlin, Germany
T.Kubo[2], High Energy Accelerator Research Organization (KEK), Tsukuba, Japan
[1]also at Universität Siegen, Siegen, Germany
[2]also at The Graduate University for Advanced Studies (Sokendai), Hayama, Japan

Abstract

A dedicated experimental setup to measure magnetic flux dynamics and trapped flux in samples is used to precisely map out how trapped flux is influenced by different parameters. The setup allows for rapid thermal cycling of the sample so that effects of cooldown parameters can be investigated in detail. We show how temperature gradient, cooldown rate, and the magnitude of external field influence trapped flux in large-grain, fine-grain and coated niobium samples. The detailed measurements show unexpected results, namely that too fast cooldowns increase trapped flux, large-grain material traps flux only when the external field is larger than a temperature gradient dependent threshold field, and the measured dependence of trapped flux on temperature gradient does not agree with an existing model. Therefore, a new model is presented which agrees better with the measured results.

INTRODUCTION

When type-I superconductors are cooled below their transition temperature a fraction of the surrounding magnetic field can be trapped in the form of quantized magnetic flux lines. The radio frequency (RF) field induced in superconducting radio frequency (SRF) cavities cause these flux lines to oscillate back and forth which dissipates power. This limits the performance of modern SRF cavities which is why they are operated in permalloy shields to reduce the earth's magnetic field. However, it is impossible to completely shield of all magnetic fields. Therefore, research is ongoing on how to improve flux expulsion in SRF cavities.

Experiments investigating trapped flux are done using either cavities or samples. Experiments using cavities have the advantage that cooldown parameters like temperature gradient during cooldown and cooldown rate can be influenced in certain limits and the increased surface resistance due to trapped flux can be measured. They have the disadvantage that experiments are very time consuming so only few data points can be recorded and they have a complex geometry which makes applying treatments more difficult compared to samples [1]. Experiments using samples like magneto optical imaging (MOI) make use of smaller samples but the experiments, so far, are limited in the adjustability of the cooldown parameters. Additionally, the magnetic flux

density required for MOI is in the range of mT, whereas the earth's magnetic field is $\approx 50\,\mu T$.

Therefore, an experimental setup was designed at HZB which measures trapped flux in flat, rectangular samples. It allows for fast thermal cycles (≈ 300 per day) and independent control of the cooldown parameters of temperature gradient across the sample during cooldown, cooldown rate, and external magnetic field. This enables the dependencies of trapped flux on these parameters to be mapped out in more detail compared to cavity measurements. Additionally, the geometry of the samples is simpler so different materials and treatments can be tested more easily, and the impact of geometry is easier to understand.

Besides the developed setup we present data gathered with different samples showing how trapped flux in influenced by temperature gradient during cooldown, cooldown rate, and external magnetic field. Finally, a phenomenological model is developed describing the dependency of trapped flux on temperature gradient and external magnetic field.

EXPERIMENTAL SETUP

Experimental Infrastructure

The experiments are conducted in a small glass cryostat which is filled via a transfer line from a helium dewar. Figure 1 shows a picture of the cryostat with two rectangular Helmholtz-coil pairs attached to the holding frame and a solenoid wrapped around the aluminum housing of the cryostat. Since the cryostat has no permalloy shielding these coils are necessary to compensate the surrounding magnetic field. With these coils and an iterative compensation scheme the flux density at the position of the reference sensors is compensated below 15 nT. COMSOL Multiphysics [2] simulations suggest a field flatness in the sample volume of 0.8% for the solenoid coil and <0.1% for the Helmholtz-coil pairs. With the current power supplies a maximum field of $180\,\mu T$ can be achieved in each direction.

Setup to Measure Flux Trapping in Flat Samples

The design of the setup follows two main goals: The first is to control the cooldown parameters of temperature gradient, and cooldown rate independently of each other. The second is to perform temperature cycles through the critical temperature quickly, so many data points can be recorded. Additionally, the sample geometry should be simple, so that geometric effects are easier to isolate and treatments are easy to apply. Furthermore, the sample should be large enough so that the measurements are not

---

* f.kramer@helmholtz-berlin.de

Figure 1: Picture of glass cryostat with two Helmholtz-coil pairs mounted to the aluminum frame creating field in x-direction (red corners) and y-direction (blue corners). Additionally, an insulated copper wire is wound around the cryostat's housing, forming a solenoid which creates field in z-direction.

dominated by edge effects and a grid of magnetic field sensors can be placed next to it.

To achieve these goals the sample geometry was chosen to be a rectangle of dimensions $(100 \times 60 \times 3)\,\text{mm}^3$. For this size, simulations suggest nearly no influence of edge effects on the measurements, and a grid of 3×5 magnetic field sensor groups can be placed next to the sample which makes it possible to study dynamic effects.

The sample is clamped in copper blocks at either end which are mounted to the cryostat's insert. A schematic depiction of the setup is shown in Fig. 2. At the far end of the copper blocks independently PID controlled electric heaters are mounted so that the temperature of the sample and the temperature gradient across the sample can be controlled. The purpose of the copper blocks is to move the electric heaters away from the sample so that any magnetic fields created by the heaters is not measurable at the sample position. Since the sample must be cycled through its transition temperature $T_c (9.2\,\text{K}$ for niobium) the setup is not submerged in liquid helium but is suspended above a helium reservoir. An additional heater in the reservoir is used to evaporate helium in a controlled manner to create a gas flow of cold helium gas to cool down the sample below 9.2 K.

To monitor the local temperature gradient on the sample 8 Cernox sensors are glued to it in a vertical line. This way any inhomogeneities in the temperature gradient are detected.

The magnetic field is measured with two different sensor types: Fluxgate and anisotropic magnetoresistive (AMR)
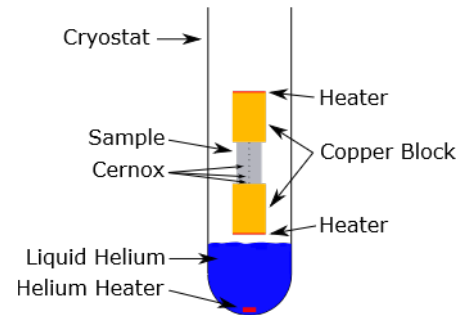

Figure 2: Schematic depiction of experimental setup in cryostat.

sensors. Three single axis Fluxgate sensors are mounted close to the sample which measure the magnetic field in 3D. They are used as reference sensors for the field compensation and to calibrate the AMR sensors. The AMR sensors are used to measure trapped flux. For this purpose they are mounted as closely as possible to the sample on a custom printed circuit board (PCB). On this board three sensors are grouped in a sensor group to measure the field in 3D. A picture of the PCB with the AMR sensors soldered on to it is depicted in Fig. 3.
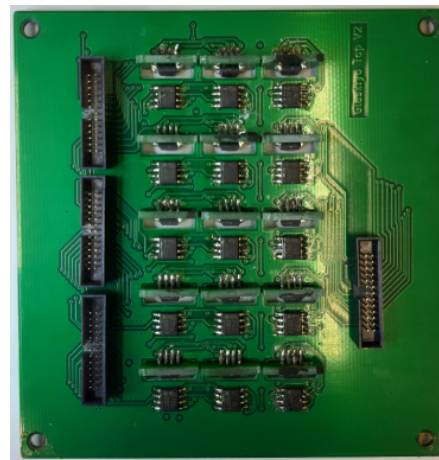

Figure 3: Picture of PCB with 15 AMR sensors groups. The sensors on the front of the board measures field in vertical direction. Sensors measuring in horizontal direction (left to right) are soldered to the back of the PCB. Sensors measuring in direction perpendicular to the paper plane are soldered to small adapter PCB which are inserted in slits on the main PCB.

Measurement Procedure

The measurements procedure is illustrated with a specific cooldown as example. In this cooldown the temperature gradient during cooldown is supposed to be $0.06\,\frac{\text{K}}{\text{cm}}$, the cooldown rate $0.07\,\frac{\text{K}}{\text{s}}$ and the external magnetic flux density $100\,\mu\text{T}$ perpendicular to the surface: First, the sample is heated above T_c with the two heaters on the copper blocks. Then, the external field is compensated to zero and the cor-

responding coil currents are stored. Once the currents are stored the external field is set to 100 µT perpendicular to the sample's surface. After that the temperature of the bottom edge of the sample is set to 9.5 K and the the temperature at the top edge to 10.1 K. Since the sample is 10 cm long this corresponds to the desired temperature gradient of 0.06 $\frac{\text{K}}{\text{cm}}$. Once the temperature is stable the set temperature for the top and bottom edge are lowered simultaneously with a rate of 0.07 $\frac{\text{K}}{\text{s}}$. This ensures a constant temperature gradient during cooldown. The sample now becomes superconducting from bottom to top. After the sample is fully superconducting the previously stored coil currents for the field compensation are set again in the coils, effectively eliminating any external field. At this point the AMR sensors measure only the magnetic flux trapped inside the sample.

RESULTS

In the following section the effect of temperature gradient, external magnetic flux density, and cooldown rate are presented. The presented results are gathered with three different samples. The first is cut out of a large-grain niobium sheet with RRR = 300 intended for cavity fabrication. It is cut such that it consists of only two grains with the grain boundary running through the center of the sample parallel to the shorter edge (60 mm). The second sample is cut out from a fine-grain sheet with RRR = 300. The grain size is around 100 µm. The third sample is niobium sputtered on a copper substrate. The niobium film has a thickness of 4 µm. It was coated by the group "Oberflächentechnik" from Universität Siegen. For the results shown here, all samples are completely untreated. This means there probably is a damaged layer on the surface of the bulk samples.

Simulations suggest that even with homogeneous distribution of magnetic flux in the sample the sensors measure different flux magnitudes depending on their position, due to the geometry of the sample. This makes averaging the measured flux densities meaningless and in the following plots only the trapped flux magnitude recorded with the central sensor group is depicted.

Temperature Gradient

To measure the effect of temperature gradient across the sample during cooldown the external magnetic field and cooldown rate are kept constant and only the temperature gradient is altered. The external magnetic field is orientated perpendicular to the large sample surface and is kept at a constant 100 µT for all cooldowns. The cooldown rate is set to 0.07 $\frac{\text{K}}{\text{s}}$. Figure 4 shows the resulting trapped flux magnitudes.

The investigation of the three samples reveal three distinct behaviors. In case of the large-grain sample the amount of trapped flux falls steeply and above a temperature gradient of ≈ 0.1 $\frac{\text{K}}{\text{cm}}$ nearly full flux expulsion is achieved. For the fine-grain sample the slope is less steep, and measurements with another fine-grain sample show that above a temperature gradient of ≈ 0.3 $\frac{\text{K}}{\text{cm}}$ no further decrease in trapped
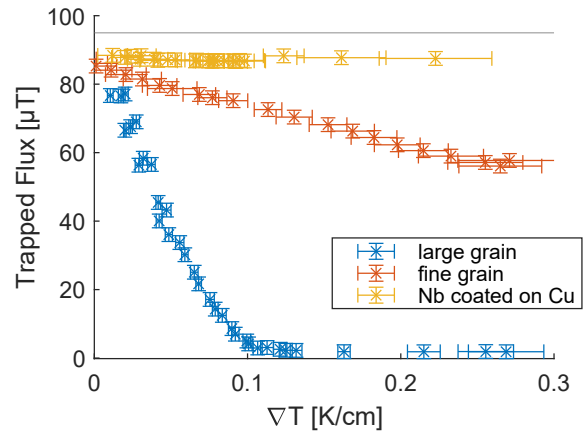

Figure 4: Trapped flux measured by the central sensor group versus temperature gradient during cooldown for three different samples. The constant line at 95 µT indicates the simulated flux density at the central sensor for 100% flux trapping. The difference arises because there is a gap between sample and sensor. The three samples behave clearly different.

flux is achieved with higher temperature gradient. The most extreme case is observed for the coated sample. Here, no dependency of trapped flux on temperature gradient is measured.

External Magnetic Field Strength

To measure the effect of the flux density magnitude on trapped flux the temperature gradient and cooldown rate are kept constant within one measurement series. The orientation of the external field is kept constant pointing at the large sample surface. The magnetic flux density is altered from -180 µT to +200 µT. Once a measurement series is completed a new series with a different temperature gradient is recorded where the flux density is again altered from -180 µT to +200 µT. The results obtained with the large-grain sample are depicted in Fig. 5.

For $\nabla T = 0 \frac{\text{K}}{\text{cm}}$ a linear increase of trapped flux with magnetic flux density is observed. For the higher gradients of $\nabla T = 0.04 \frac{\text{K}}{\text{cm}}$, and $\nabla T = 0.1 \frac{\text{K}}{\text{cm}}$ flux is only trapped when the external magnetic flux density exceeds a threshold field. Once flux start to get trapped the increase, again, seems to be linear. The threshold field depends on the temperature gradient, where a larger gradient leads to a larger threshold field. This is investigated in more detail further below.

Cooldown Rate

Lastly, the effect of cooldown rate on trapped flux is presented. For these measurements the external magnetic flux density is kept constant at 100 µT pointing at the large sample surface and the temperature gradient is constant within one series. The cooldown rate is then altered between cooldowns. Figure 6 depicts trapped flux versus transition time. Transition time denotes the time it takes the sample to become fully
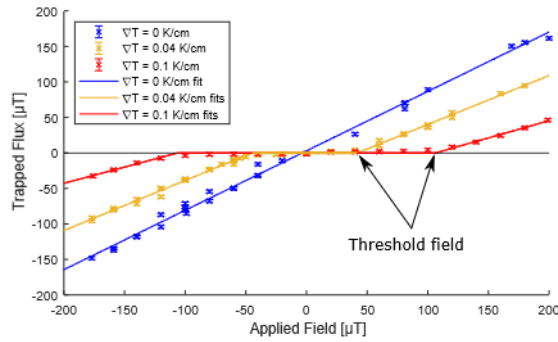
Figure 5: Trapped flux measured by the central sensor group versus flux density. The orientation is kept constant, pointing at the large sample surface. The different series show the response for different temperature gradients during cooldown. For non-zero temperature gradients flux is only trapped once a certain threshold field is reached.

superconducting once it starts at the bottom. In practice it is the time difference between the point when the lowest and highest temperature sensor pass 9.2 K.
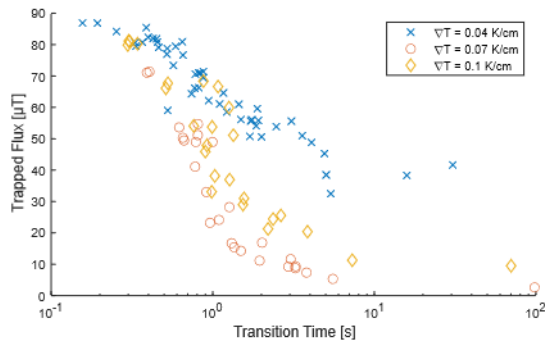

Figure 6: Trapped flux measured by the central sensor group versus transition time. The different measurement series investigate the dependency at different temperature gradient. At small transition times trapped flux becomes nearly independent of temperature gradient. Note the logarithmic x-scale.

It is evident that even at a high temperature gradient of $\nabla T = 0.1\,\frac{K}{cm}$ nearly all flux is trapped at very short transition times. Trapped flux then sharply decreases up to a transition time of $\approx 1\,s$ after which a slower decrease up to $\approx 7\,s$ is noticeable. For even longer transition times no effect is visible anymore.

MODELING TRAPPED FLUX

In this section the basic idea of the model is explained first. Then the gathered data is used to refine the model and the result is applied to the large-grain and fine-grain sample. The described model is still in development and there are still questions to be resolved. The model is described in a bit more detail in these proceedings in SUSPB017.

Base Model

The model picks up on in ideas from the model in Ref. [3]. Since the measurements are conducted in an external magnetic field, and a temperature gradient is established across the sample it is in three states simultaneously during cooldown. This is schematically shown in Fig. 7
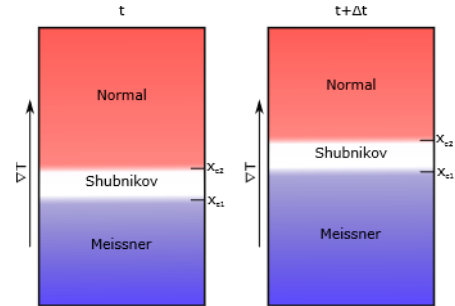

Figure 7: During transition the sample is in three sates simultaneously: Below x_{c1} the sample is cold enough so that the external field is smaller than B_{c1}. Between x_{c1} and x_{c2} the sample is in the mixed state. Above x_{c2} the sample is still normal conducting. During cooldown the transition region moves up the sample.

While the transition region is moving up the sample during cooldown magnetic flux enters the mixed state at x_{c2} where quantized flux lines are established. While the flux lines are in the mixed domain they are pushed by the thermal force [4] towards the Meissner state at x_{c1}. While the flux lines move through the domain in the mixed state they encounter pinning centers. It is assumed that the pinning center density is high so that each flux line interacts with at least one pinning center. Depending on whether the thermal force is smaller or larger than the pinning force of a given pinning center a flux line gets either pinned or not. At this point the dynamics of the flux line movement at the transition to the Meissner state at x_{c1} is not clear but it is assumed that flux lines get trapped in the sample if they are at a position of a pinning center (i.e. they are pinned) when x_{c1} reaches them, if not they are expelled. If the thermal force is larger than the pinning force they are pushed over the pinning centers so they can be expelled when the Meissner state reaches them.

Since the thermal force is proportional to the temperature gradient [4] it can be expressed as $f_{th} = a\nabla T$ with a constant a. If the thermal force is larger than the pinning force (f_p) of all pinning centers it encounters the flux line is expelled. Since the pinning force of all pinning centers is not known a density distribution function $n(f_p)$ is introduced which describes the probability of a pinning center to interact with a pinning center with pinning force f_p. It is normalized to fulfill $\int_0^\infty n(f_p)\mathrm{d}f_p = 1$. The distribution function is not known and Fig. 8 shows a hypothetical example of how it might look like. Since different pinning centers might have different underlying pinning mechanism, like for example grain boundaries, crystalline defects, or normal conducting inclusions, it is not continuous. The extreme pinning forces that can be reached by the different mechanisms are label f_1

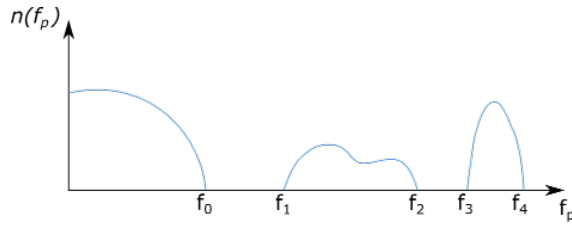to f_4. The ratio r_{trap} of flux lines that get pinned depend on

Figure 8: Hypothetical density distribution $n(f_{\text{p}})$. Due to different pinning mechanism it is not continuous. The most extreme forces reachable by a mechanism are label f_1 to f_4.

how strong the thermal force is compared to the distribution function. r_{trap} can also be expressed in terms of the ratio of flux lines that get expelled (r) as $r_{\text{trap}} = 1 - r$ where

$$r(\nabla T) = \int_{f_{\text{p}} < f_{\text{th}}} n(f_{\text{p}}) \mathrm{d}f_{\text{p}}. \tag{1}$$

Equation (1) incorporates that flux lines get expelled when the pinning force is smaller than the thermal force. At this point two assumptions are made in order to make predictions from this model:

1. The maximal reachable thermal force is larger than f_0 but smaller than f_1: $f_0 < f_{\text{th max}} < f_1$.

2. The distribution function is constant below f_0: $n(f_{\text{p}} < f_0) = n_0 = const$.

The second assumption is only made for now to illustrate the underlying model. This assumption will be relaxed further below. Using these assumptions r can be calculated:

$$r(\nabla T) = \int_{f_{\text{p}} < f_{\text{th}}} n(f_{\text{p}}) \mathrm{d}f_{\text{p}}$$
$$= n_0 a |\nabla T| \left[1 - \theta \left(|\nabla T| - \frac{f_0}{a} \right) \right] + n_0 f_0 \theta \left(|\nabla T| - \frac{f_0}{a} \right)$$
$$= k |\nabla T| \left[1 - \theta \left(|\nabla T| - \frac{R_w}{k} \right) \right] + R_w \theta \left(|\nabla T| - \frac{R_w}{k} \right).$$

Here, θ is the heaviside step function, and $k = n_0 a$, and R_w are fit parameters. R_w is the ratio of weak pinning centers: $R_w = \int_{f_{\text{p}} < f_0} n(f_{\text{p}}) \mathrm{d}f_{\text{p}} = n_0 f_0$. To calculate the trapped flux magnitude (B_{TF}) r_{trap} is multiplied with the external flux density:

$$B_{\text{TF}} = (1 - r(\nabla T)) B_{\text{e}} \tag{2}$$
$$= B_{\text{e}} - B_{\text{e}} \left[k |\nabla T| \left[1 - \theta \left(|\nabla T| - \frac{R_w}{k} \right) \right] \right.$$
$$\left. + R_w \theta \left(|\nabla T| - \frac{R_w}{k} \right) \right]. \tag{3}$$

This results in a linear decrease of trapped flux starting at 100% trapped flux at $\nabla T = 0 \frac{\text{K}}{\text{cm}}$. Once a temperature gradient of $\frac{R_w}{k}$ is reached a constant level of trapped flux is predicted. Figure 9 shows measurement results obtained
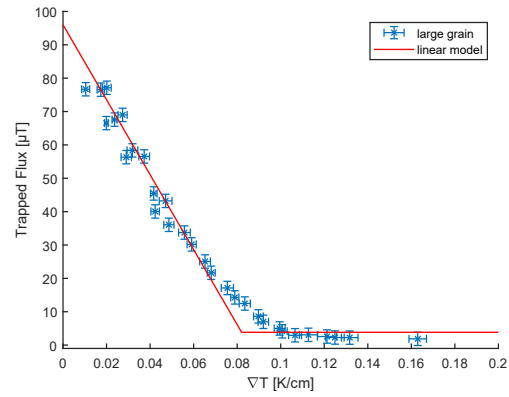

Figure 9: Measurement results gained from the large-grain sample and fit results according to Eq. (3).

from the large-grain sample together with a fit according to Eq. (3).

Figure 9 shows good agreement between fit and measurement data. However, the curvature that is noticeable in the measurement data is not represented in the model. Therefore, trapped flux versus external magnetic field data is analyzed in more detail in the following subsection to refine the model.

Refining the Model

In order to refine the model the second assumption that $n(f_{\text{p}})$ is constant for forces smaller f_0 is dismissed. To predict how the distribution function might look like the trapped flux versus external magnetic flux density data is analyzed in more detail. Figure 10 depicts measurement results obtained with the large-grain sample.
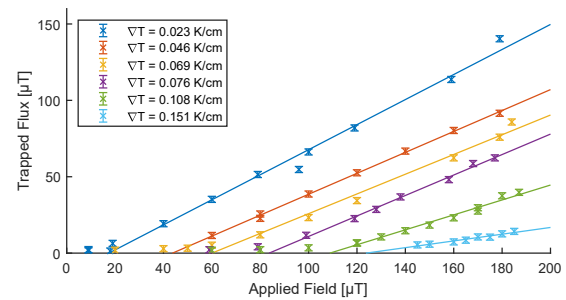

Figure 10: Trapped flux magnitude versus external magnetic flux density. Measurement series at different temperature gradients are depicted and color coded. Measurement points of the same series are fitted with linear regression. The fit results are displayed in the same color.

Since the trapped flux magnitude seems to be increasing linearly with increasing field level once flux starts to get trapped a linear fit is performed for all data points recorded at the same temperature gradient and above the threshold field. The results of these fits are also displayed in Fig. 10. The color of the fit matches the color of the data points.

The obtained fit parameters from the linear fits can now be plotted versus the mean temperature gradient of the data points used for the respective fit. Figure 11 depicts the slope η of the fits versus temperature gradient. For better readability not all recorded measurement series are depicted in Fig. 10 which is why there are more points in Figs. 11–13 than there are fits depicted in Fig. 10.
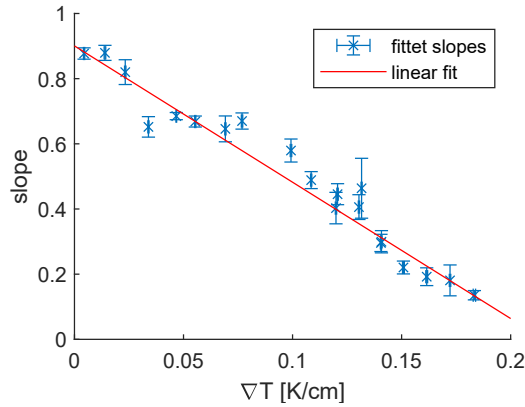

Figure 11: Slope of linear fits in Fig. 10 versus mean temperature gradient of data points used for the fit. In Fig. 10 not all measured series are depicted for better readability which is why this plot shows more slopes than there are fits in Fig. 10.

At this point an assumption is made that the slope η decreases linearly with temperature gradient so that it can be parameterized as

$$\eta(|\nabla T|) = \eta_0 \left(1 - \frac{|\nabla T|}{g_c}\right). \qquad (4)$$

Here, η_0 is the expulsion efficiency at $\nabla T = 0 \frac{K}{cm}$, and g_c is a critical temperature gradient at which the slope becomes 0. A fit according to Eq. (4) is also depicted in Fig. 11.

Figure 12 shows the x-axis crossings of the linear fits in Fig. 12. This x-axis crossing equals the threshold field (B^*) where flux starts to get trapped. Here it is again assumed that B^* increases linearly with temperature gradient. It is parameterized as

$$B^*(|\nabla T|) = b\frac{\nabla T}{g_c}. \qquad (5)$$

Here, b is the sensitivity of the threshold field to changes in temperature gradient. Figure 12 shows the resulting fit according to Eq. (5).

In Fig. 12 it is noticeable that the threshold field does not seem to be increasing above a gradient of $\nabla T \approx 0.13 \frac{K}{cm}$. However, at this point the error bars also increase strongly. This is caused by the limitations of the setup because at high gradients high magnetic field strengths are needed in order to trap flux. But since the setup is limited at $\approx 190 \, \mu T$ only few data points can be obtained. Additionally, the ones that are obtained show low magnitudes of trapped flux which makes measurement errors more significant. This behavior can be
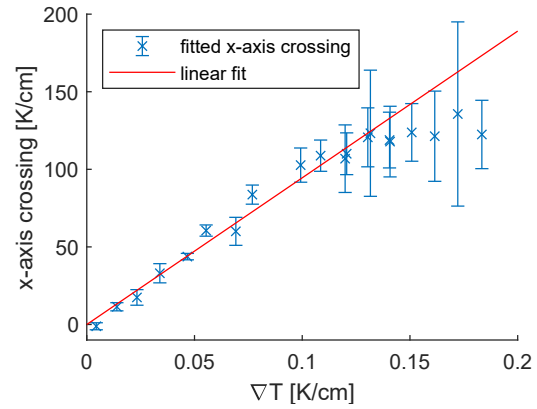

Figure 12: x-axis crossing, or threshold field (B^*), of linear fits in Fig. 10 versus mean temperature gradient of data points used for the fit. In Fig. 10 not all measured series are depicted for better readability which is why this plot shows more data points than there are fits in Fig. 10.

seen in Fig.10 where at the highest gradient the recorded data points are close together and also close to zero.

With the prior two assumptions that the slope and threshold field decrease or increase linearly with temperature gradient respectively it follows that the y-axis crossing in Fig. 10 must have a quadratic term in its dependency on the temperature gradient. In order to check this the y-axis crossings of the fits in Fig. 10 are plotted against temperature gradient in Fig. 13. Additionally, the expected value using the two prior assumptions (Eq. (4), Eq. (5)) is depicted in red. Figure 13 clearly shows a quadratic dependence of the y-axis crossing which reinforces the two assumptions.
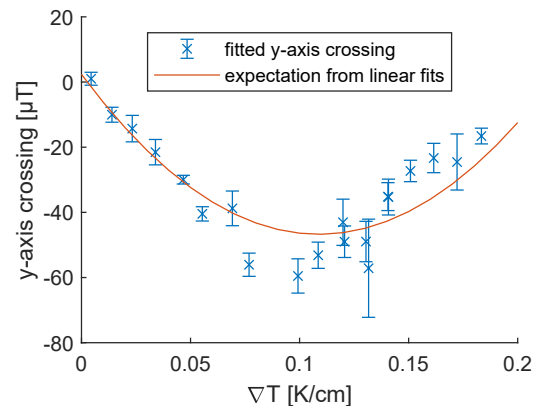

Figure 13: y-axis crossing of linear fits in Fig. 10 versus mean temperature gradient of data points used for the fit. A quadratic dependency on temperature gradient is clearly visible. The prediction from Eqs. (4) and (5) is plotted in red. In Fig. 10 not all measured series are depicted for better readability which is why this plot shows more data points than there are fits in Fig. 10.

To summarize three assumptions were made up to this point:

1. The dependence of trapped flux on applied field magnitude is linear once flux starts to get trapped above B^* (Fig. 10).

2. The slope of the linear fits in 1. decreases linearly with increasing temperature gradient (Fig. 11).

3. The x-axis crossing, or B^*, increases linearly with increasing temperature gradient (Fig. 12).

Using these three assumptions the ratio of expelled flux lines, and the resulting trapped flux magnitude can be calculated again similar to what is shown above. The derivation cannot be shown here and only the result is stated. For more details see SUSPB017 in these proceedings or [5].

$$B_{\text{TF}}(B_{\text{e}}, \nabla T) =$$
$$\eta_0 B_{\text{e}} - \left\{ \left[-\eta_0 b \left(\frac{|\nabla T|}{g_{\text{c}}} \right)^2 + \eta_0 (B_{\text{e}} + b) \frac{|\nabla T|}{g_{\text{c}}} \right] \times \right.$$
$$[1 - \theta(|\nabla T| - \kappa)] +$$
$$\left. \left[-\frac{\eta_0 b}{g_{\text{c}}^2} \kappa^2 + \frac{\eta_0}{g_{\text{c}}} (B_{\text{e}} + b) \kappa \right] [\theta(|\nabla T| - \kappa)] \right\}. \quad (6)$$

Here, $\kappa = \frac{f_0}{a}$ is the temperature gradient at which the thermal force equals f_0 and above it trapped flux stays constant. In Eq. (6) a quadratic correction term is introduced compared to the previous result in Eq. (3).

Equation (6) can now be fitted to trapped flux versus temperature gradient data with a constant external magnetic flux density of $100\,\mu\text{T}$. Using the obtained fit parameters the model can then be used to predict trapped flux at different external flux densities. This is shown in Fig. 14. However, in order to predict the trapped flux correctly κ must be scaled linearly with the external flux density. Since the origin of the threshold field is not yet understood the scaling of κ cannot be physically explained at this point.

Figure 15 shows the same data as Fig. 14 but for the fine-grain sample.

CONCLUSION AND OUTLOOK

The measurement results obtained with this setup showed both expected and unexpected results: It is observed that higher temperature gradients lead to less trapped flux, and that large-grain material expels flux more efficiently that fine-grain material. For the large-grain sample nearly full expulsion is observed. These results could be expected from earlier experiments [6,7] but in case of the large-grain sample it is observed that flux only gets trapped above a temperature gradient dependent threshold field which, to our knowledge, has not been reported previously. Furthermore, we find that the efficacy of higher temperature gradients diminishes if the cooldown rate is too fast.

With the obtained data a new model is developed which shows good agreement with the data and can predict trapped flux magnitude at different external flux densities and temperature gradients. This model is, however, still in an early
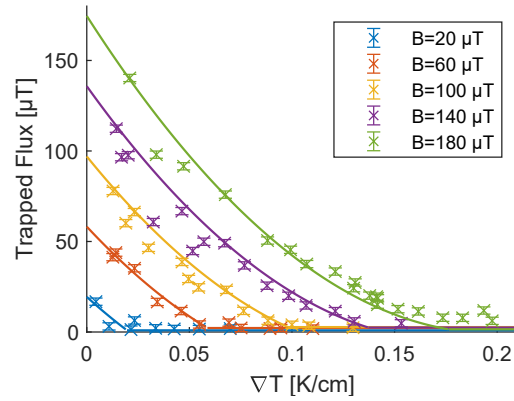

Figure 14: Trapped flux versus temperature gradient data obtained with the large-grain sample at different external magnetic flux densities. Equation (6) is fitted to the data recorded at $100\,\mu\text{T}$. The obtained fit parameters are used to predict trapped flux at different external flux densities (solid lines).
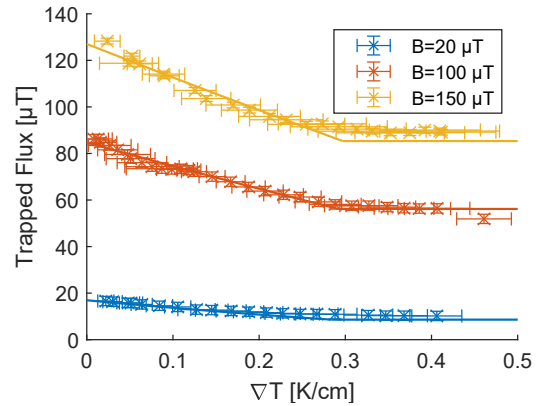

Figure 15: Trapped flux versus temperature gradient data obtained with the fine-grain sample at different external magnetic flux densities. Equation (6) is fitted to the data recorded at $100\,\mu\text{T}$. The obtained fit parameters are used to predict trapped flux at different external flux densities (solid lines).

stage and there are still many open questions. It is for example still not understood what the flux line dynamics at the Meissner phase transition front are, and how the threshold field B^* arises.

In the future, more experiments with other materials and material treatments are planned. The gathered data hopefully opens new insights in the open questions so the model can be further refined.

REFERENCES

[1] F. Kramer, O. Kugeler, J.-M. Köszegi, and J. Knobloch, "Impact of geometry on flux trapping and the related surface resistance in a superconducting cavity", *Phys. Rev. Accel. Beams*, vol. 23, p. 123101, Dec. 2020.
doi:10.1103/PhysRevAccelBeams.23.123101

[2] COMSOL AB, Comsol multiphysics v. 6.0, 2021.
`http://www.comsol.com`

[3] T. Kubo, "Flux trapping in superconducting accelerating cavities during cooling down with a spatial temperature gradient", *Prog. Theor. Exp. Phys.*, vol. 2016, p. 053G01, 2016.
`doi:10.1093/ptep/ptw049`

[4] R. P. Huebener, "Superconductors in a temperature gradient", *Supercond. Sci. Technol.*, vol. 8, no. 4, pp. 189–198, 1995.
`doi:10.1088/0953-2048/8/4/001`

[5] F. Kramer, "Impact of cooldown conditions on trapped flux in superconducting niobium", Ph.D. dissertation, Universität Siegen, to be published.

[6] A. Romanenko *et al.*, "Ultra-high quality factors in superconducting niobium cavities in ambient magnetic fields up to 190 mG", *Appl. Phys. Lett.*, vol. 105, p. 234103, 2014.
`doi:10.1063/1.4903808`

[7] S. Huang, T. Kubo, and R. Geng, "Dependence of trapped-flux-induced surface resistance of a large-grain Nb superconducting radio-frequency cavity on spatial temperature gradient during cooldown through T_c", *Phys. Rev. Accel. Beams*, vol. 19, p. 082001, Aug. 2016.
`doi:10.1103/PhysRevAccelBeams.19.082001`

Fundamental SRF research and development

High quality factors/high gradients